

# **pesc98<sup>®</sup>**

## **RECORD**

### **VOLUME 2**

29th Annual  
IEEE Power Electronics Specialists Conference

*Formerly*  
POWER CONDITIONING SPECIALISTS CONFERENCE 1970-71  
POWER PROCESSING AND ELECTRONIC SPECIALISTS CONFERENCE 1972

---

The 1998 PESC is Sponsored by the

**IEEE POWER ELECTRONICS SOCIETY**



and the  
**IEICE OF JAPAN**



In cooperation with the  
**IEEJ**  
and the  
**IEI OF JAPAN**

98CH36196

# SDI (Strategic Dual Image) solution of PCB (Printed Circuit Board) containing magnetic material

Fabienne Cortial

NEC Europe Ltd., C&C Research Laboratories  
 Rathausallee 10, 53757 Sankt Augustin, Germany  
 Tel: 49/(0) 2241/9252-0; Fax: 49/(0) 2241/9252-99;  
 Email : cortial@crrl-nece.technopark.gmd.de

Shiro Yoshida, Hirokazu Tohya  
 NEC Corporation, Kanagawa, Japan

Yoichi Midorikawa, Yoshifuru Saito  
 Hosei University, Tokyo, Japan

## ABSTRACT

One way to control electromagnetic interference (EMI) generated on a printed circuit board (PCB) operating at high frequency is to cover the power layer by a magnetic thin film. The device modeling makes it possible to analyze electromagnetic features and then to optimize the device performances. This paper presents the finite element modeling of a 2D axisymmetric, magnetodynamic, unbounded problem composed by a PCB containing a Mn-Zn ferrite thin film. Hysteresis is taken into account in the computation. The final solution is obtained by using the Strategic Dual Image method (SDI). The results show especially the good performances of this device configuration at high frequency, up to 1 GHz.

## 1. INTRODUCTION

Recently, radiated emission noise on Printed Circuit Board (PCB) operating at high frequency is become an important problem because of the consequential degradation of the device performances. One convenient way to prevent this electromagnetic interference (EMI) generation is to coat the PCB power layer by a thin magnetic material with appropriate properties. Then the modeling by the finite element method (FEM) permits to optimize the device configuration by evaluating numerically the global electromagnetic features such as the magnetic field, the inductance, the eddy currents and the losses.

The aim of this work is to present an original methodology of high frequency PCB performance analysis and to apply it to a simple PCB configuration including a magnetic material. The study especially shows the importance of the modeling in the new PCB development. However, this approach requires a representation of the problem physics, and particularly the magnetic film behavior, as accurate as possible. Among the published hysteresis models [1-2], a Chua-type model is chosen since it offers a good compromise between accuracy and simplicity [3-4]. The FEM

permits to model the device. As it solves only bounded problems, it can not directly be applied. By consequence, the strategic dual image method (SDI) is used in this work in order to obtain the finite element solution of the open boundary problem [5-6]. This methodology has already been applied to a similar device and good results have been obtained [7].

The PCB configuration of the present work is a power layer covered by a soft ferrite thin film. A 2D modeling is investigated because the device contains an axial symmetry. The problem is magnetodynamic and accounts for hysteresis. By symmetry, only a quarter part of the device is modeled, as shown in Fig. 1. The geometric and physical problem parameters are defined in Table 1. The problem solving makes it possible to compute the magnetic field and then to deduce inductance, eddy current and hysteresis losses. A frequency analysis permits to conclude about the configuration performances.

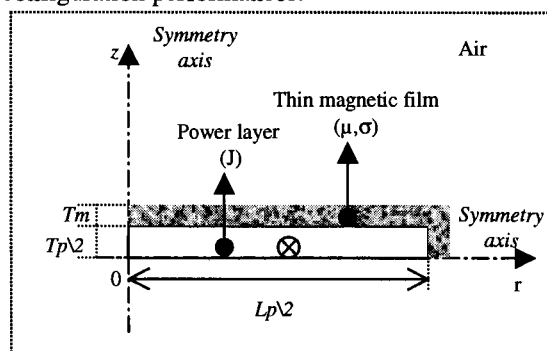


Fig. 1. Problem configuration

TABLE 1  
 Problem parameter definition

r,z	Axisymmetric coordinates
Tp	Power layer thickness
Lp	Power layer diameter
Tm	Magnetic film thickness
J	Power layer current density
μ	Magnetic film permeability
σ	Magnetic film conductivity

## 2. MAGNETIC THIN FILM STUDY

### 2.1. The magnetization model: a complex permeability derived from a Chua-type model

Accounting for hysteresis accurately is essential to study properly the device magnetic behavior at high frequency. A suitable model must not only represent properly magnetic hysteresis, but also require few parameters and be relatively simple for its implementation in the computation. The Chua-type model given by (1) fulfils these requirements [3]. Based on the magnetic domain theory, it links the magnetic field intensity  $H$ , the magnetic flux density  $B$  as well as their respective time derivatives  $dH/dt$  and  $dB/dt$ . It contains three parameters which are the permeability  $\mu_p$ , the reversible permeability  $\mu_r$  and the hysteresis parameter  $s$ . Moreover, it has been shown that this model takes anomalous eddy currents into account by the coefficient  $s$  [3].

$$H = \left( \frac{1}{\mu_p} \right) B + \left( \frac{1}{s} \right) \frac{dB}{dt} - \left( \frac{\mu_r}{s} \right) \frac{dH}{dt} \quad (1)$$

Since the flux density peak in magnetic film remains sufficiently small at high frequency, both following assumptions are considered:

- the magnetic field intensity  $H$  and flux density  $B$  are assumed to vary sinusoidally with time.
- the model parameters  $\mu_p$ ,  $\mu_r$  and  $s$  are constant.

These conditions permit to derive from (1) a complex permeability given by (2). Its real and imaginary parts are expressed as a function of the parameters  $\mu_p$ ,  $\mu_r$ ,  $s$  and the angular frequency  $\omega$  ( $\omega=2\pi f$ , with  $f$  the problem frequency),  $j$  representing the imaginary number ( $j = \sqrt{-1}$ ).

$$\mu(\omega) = \frac{B}{H} = \mu_{Re}(\omega) - j\mu_{Im}(\omega) \quad \text{with} \quad (2)$$

$$\begin{cases} \mu_{Re}(\omega) = \frac{\mu_p (s^2 + \omega^2 \mu_p \mu_r)}{s^2 + \omega^2 \mu_p^2} \\ \mu_{Im}(\omega) = \frac{\mu_p \omega s (\mu_p - \mu_r)}{s^2 + \omega^2 \mu_p^2} \end{cases}$$

Finally, a simple complex permeability model, easy to implement, has been obtained. It represents elliptic hysteresis loops and requires three parameters  $\mu_p$ ,  $\mu_r$ ,  $s$  which are easily deduced from the experimental frequency characteristics of complex permeability [4].

### 2.2. The magnetic thin film: a Mn-Zn ferrite

For the purpose of minimizing electromagnetic noise at high frequencies, the required magnetic film must have a relatively high permeability to increase the equivalent circuit inductance as well as a relatively low

conductivity to minimize the eddy current development. Both requirements are satisfied by the 3S1 Phillips Components Mn-Zn ferrite, chosen among a wide choice of soft magnetic materials [8]. The conductivity of this ferrite film is  $\sigma=3S/m$ . The model parameters are determined by matching the computed complex permeability with the experimental corresponding characteristics. Table 2 gives the deduced parameter values and Fig. 2 represents the modeled complex permeability with some experimental data, as a function of frequency. A good agreement between model and experiment is obtained.

TABLE 2  
Model parameters of a Mn-Zn ferrite

Permeability	Reversible permeability	Hysteresis parameter
$\mu_p$	$\mu_r$	$s$
8 mH/m	0.8 mH/m	50 kΩ/m

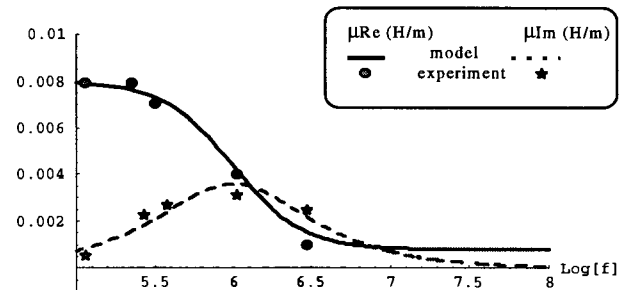


Fig. 2. Frequency characteristics of complex permeability for 3S1 Phillips Components Mn-Zn ferrite.

## 3. SOLUTION OF OPEN BOUNDARY MAGNETIC FIELD PROBLEM BY THE STRATEGIC DUAL IMAGE METHOD

### 3.1. Problem formulation

The studied device is considered as a 2D axisymmetric, magnetodynamic, open boundary problem, operating at high frequencies. It is described by:

- the Maxwell's equations :

$$\nabla \times \vec{H} = \vec{J} \quad (3)$$

$$\nabla \times \vec{E} = -\frac{d\vec{B}}{dt} \quad (4)$$

$$\nabla \cdot \vec{B} = 0 \quad (5)$$

where  $H$  denotes the magnetic field,  $B$  the magnetic induction,  $E$  the electrical field and  $J$ , the source current density,

- the linear magnetic law :  $B = \mu H$  (6)  
 $\mu$  being the permeability,

- the Ohm's law:  $\vec{J} = \sigma \vec{E}$  (7)  
 $\sigma$  being the electrical conductivity.

Equation (5) permits to define the problem state variable which is the magnetic vector potential  $\vec{A}$ , defined by:

$$\vec{B} = \nabla \times \vec{A} \quad (8)$$

$\vec{A}$  is completely determined by fixing its divergence. The Coulomb's gauge ( $\nabla \cdot \vec{A} = 0$ ) is used in this study. Then the differential equation to solve is given by (9).

$$\nabla \times \frac{1}{\mu} \nabla \times \vec{A} + \sigma \frac{d\vec{A}}{dt} = \vec{J} \quad (9)$$

The cylindrical coordinate system  $(r, \theta, z)$  is used to describe the axisymmetric problem. The vector potential  $\vec{A}$  as well as the current density  $\vec{J}$  are normal (direction  $\theta$ ) to the study plane  $(r, z)$ . Thus, (9) can be written:

$$\frac{\partial}{\partial r} \left[ \frac{1}{\mu} \frac{\partial (rA_\theta)}{\partial r} \right] + \frac{\partial}{\partial z} \left[ \frac{1}{\mu} \frac{\partial (rA_\theta)}{\partial z} \right] + \frac{\sigma}{r} \frac{\partial (rA_\theta)}{\partial t} = J_\theta \quad (10)$$

The consideration of the new state variable  $A^* = 2\pi r A_\theta$ , makes the solving of (10) easier. Regarding the assumption of sinusoidally time-varying current, the complex notation is used and the complex permeability presented in section 2-1 is introduced in (10). This leads to the final equation to solve:

$$\frac{1}{\mu(\omega)} \left\{ \frac{\partial}{\partial r} \left[ \frac{1}{2\pi r} \frac{\partial A^*}{\partial r} \right] + \frac{\partial}{\partial z} \left[ \frac{1}{2\pi r} \frac{\partial A^*}{\partial z} \right] \right\} + \frac{j\omega\sigma}{2\pi r} A^* = J_\theta \quad (11)$$

### 3.2. Strategic Dual Image method

In the finite element method, the 2D domain is decomposed in a set of geometrically simple parts (the finite elements). Then, (11) is interpolated on each element by a linear function which only depends on the  $A^*$  values at the element vertices (the nodes) and on the shape functions  $\alpha_i$ . By applying the variational method, the matrix system given by (12) is obtained.

$$[S][A^*] = [T] \quad (12)$$

[S] is a positive definite matrix and [T] a vector with the respective following general complex terms:

$$S_{ij} = \frac{1}{2\pi r_e} \iint_{domain} \left\{ \frac{1}{\mu(\omega)} \nabla \alpha_i \cdot \nabla \alpha_j + j\omega\sigma \alpha_i \alpha_j \right\} dr dz \quad (13)$$

$$T_{ij} = \iint_{domain} J_\theta \alpha_i dr dz$$

where :

- $\alpha_i(r, z)$  are the shape functions
- $\{i, j\} \in \{1, N\}^2$  with N, the node number of the problem

-  $r_e$  is the distance between axis ( $r=0$ ) and gravity center of each finite element.

The state variable values on each node, deduced from (12), verify the differential equation of the problem as well as the conditions on the domain boundary.

In the classical FEM, the magnetic field far away from the problem source is neglected and problems are bounded. However, this approximation is not valid in open boundary problems in which domain extends to infinity. A new approach is consequently required to compute the solution in the whole of the plan. The Strategic Dual Image (SDI) method, based on the electrical image method, has been proposed to solve efficiently electromagnetic problems containing ferromagnetic materials or not [5-6].

Basically, this method consists of decomposing any vector field as a sum of a rotational field and a divergent field. Both components are computed by respectively imposing the rotational field and the divergent field source images. This leads to define a 'hypothetic boundary' on which suitable conditions are set. In axisymmetric electromagnetic problems, the hypothetic boundary is elliptic, with the unique axial ratio 1.815, and the problem is solved by the FEM with two different conditions on this boundary: zero condition ( $A^* = 0$ ) and symmetrical condition ( $\frac{\partial A^*}{\partial n} = 0$ ). The average of both resulting vector potentials gives the unique problem solution.

## 4. PCB DEVICE MODELING AND SIMULATION RESULTS

### 4.1. PCB modeling

In the modeled problem shown in Fig. 1, the power layer is a conductor plate entirely covered by the proposed Mn-Zn ferrite film. The device parameters are collected in Table 3. The modeled problem is enclosed by an elliptic boundary and regularly meshed by using first order triangular finite elements. The mesh is composed by 1413 nodes and 2673 finite elements. The mesh pace being equal to  $17.5\mu\text{m}$ , the magnetic film contains 5 lines of elements.

TABLE 3  
Problem properties

➤ Power layer	
Geometrical properties	Physical properties
Diameter $L_p = 700\mu\text{m}$	Total current $I = 0.17\text{A}$
Thickness $T_p = 35\mu\text{m}$	
➤ Magnetic thin film: Mn-Zn ferrite	
Geometrical properties	Physical properties
Thickness $T_m = 87.5\mu\text{m}$	Conductivity $\sigma = 3\text{S/m}$
	Permeability $\mu = 8\text{mH/m}$
	Reversible permeability $\mu_r = 0.8\text{mH/m}$
	Hysteresis parameter $s = 50\text{k}\Omega/\text{m}$

The finite element program is worked out by using the Mathematica language. All the simulations are carried out on a 8500/150 Power Macintosh and the problem simulation for a given frequency takes one hour.

#### 4.2. Simulation results

Frequencies ranging from 100kHz to 1000MHz are investigated. For each studied frequency, the magnetic field distribution is studied as well as BH loops. Moreover, the problem inductance, the hysteresis and eddy current losses are computed.

##### ◆ Magnetic field distribution

In Fig. 3, the magnetic field distribution resulting on the one hand from the power layer without magnetic film and on the other hand from the entire device at the frequencies  $f=10\text{MHz}$  and  $f=1\text{GHz}$  is shown. In the frequency range, the magnetic equipotential lines remain concentrated in the magnetic film.

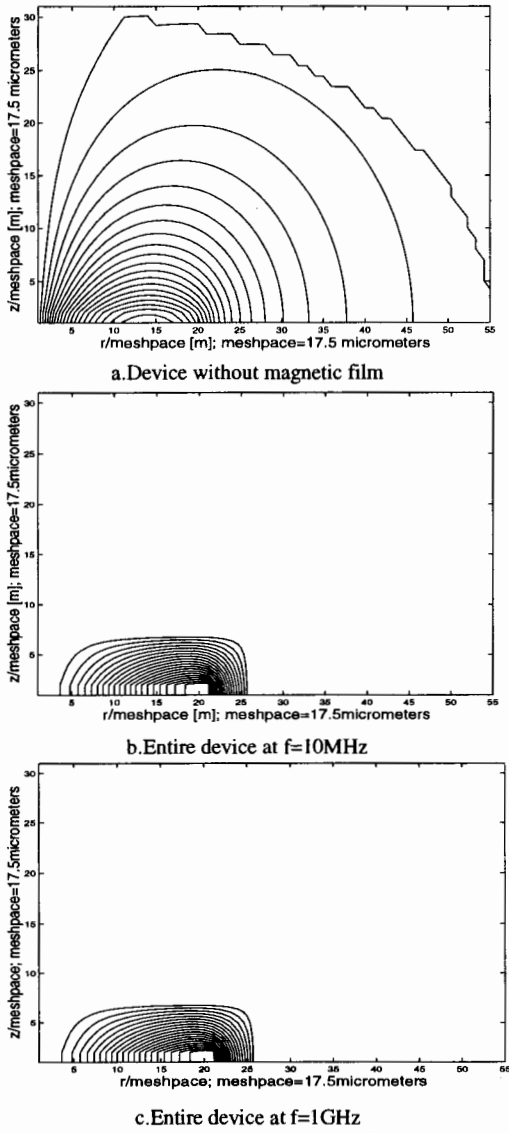


Fig. 3. Magnetic field distribution

##### ◆ BH loops

The loops  $B(H)$  of one magnetic film finite element are represented in Fig. 4 for various frequencies.

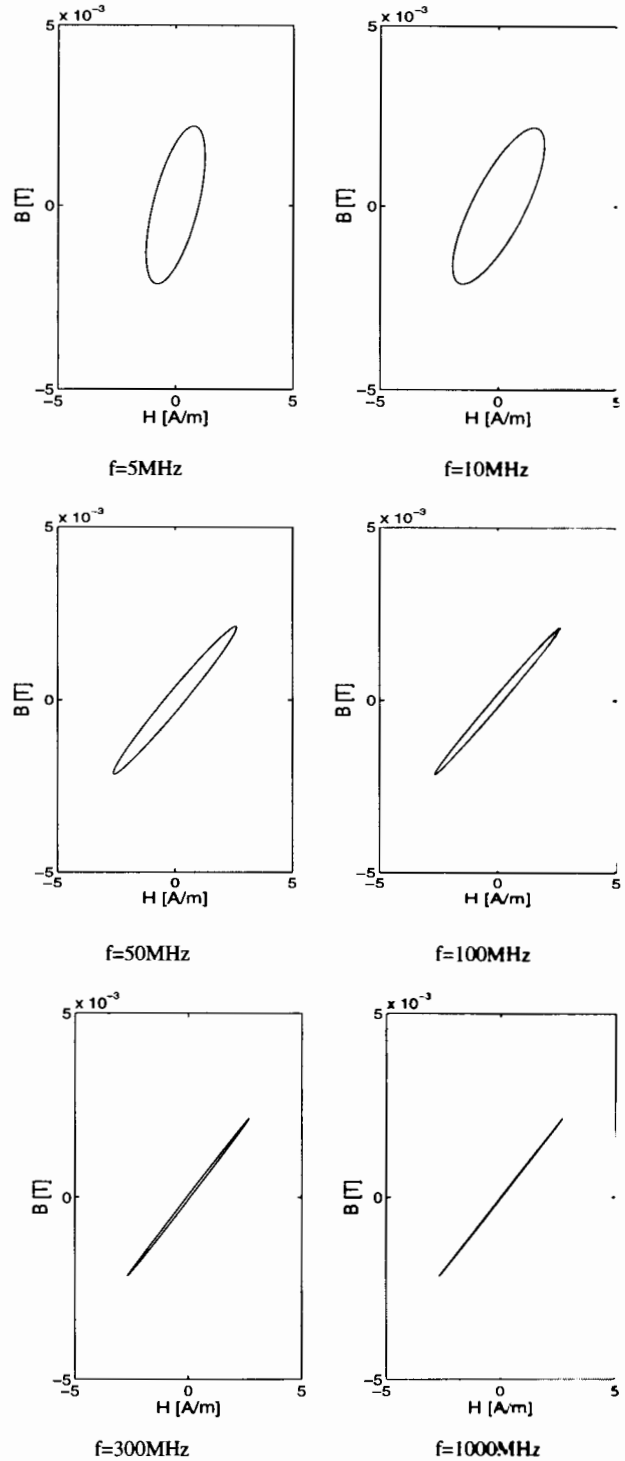


Fig. 4. Hysteresis loops for different frequencies

##### ◆ Inductance

The inductance, given by (14), is computed from the total magnetic energy expression and the total current flowing in the power layer. The quantity  $d\tau = 2\pi r dr dz$

denotes the elementary volume in the  $(r,\theta,z)$  cylindrical coordinate system.

$$\frac{1}{2}LI^2 = \left| \frac{1}{2} \iiint_{space} \vec{B} \cdot \vec{H} d\tau \right| \quad \text{with} \quad I = \iint_{power\ layer} J \cdot dr dz \quad (14)$$

Fig. 5 shows the normalized inductance variations with frequency,  $L_0$  representing the inductance of the PCB power layer without magnetic material ( $L_0=0.44\text{nH}$ ). In the studied frequency range, the inductance remains quite constant and is increased by a factor 10, compared with the device without Mn-Zn ferrite layer.

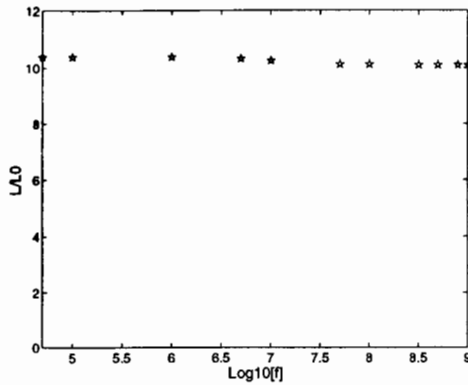


Fig.5. Frequency characteristic of the inductance

#### ◆ Losses

The hysteresis losses  $P_h$  and the eddy currents losses  $P_e$  are given by (15), per unit volume,  $V$  denoting the magnetic film volume. The hysteresis losses  $P_h$  correspond to the energy lost during each cycle. The eddy current losses result from the macroscopic eddy currents provided by the alternating magnetic flux in the magnetic film,  $J_e$  being the eddy current density  $J_e = -j\omega\sigma A$ .

$$P_h = \frac{1}{V} \iiint_V [\oint B \cdot dH] d\tau \quad P_e = \frac{1}{V} \left[ \iiint_V \frac{|J_e|^2}{\sigma} d\tau \right] \quad (15)$$

By assuming a sinusoidal steady state, the hysteresis losses are computed by using the complex permeability expression. If  $H_{max,i}$  is the maximum field intensity in the  $i^{\text{th}}$  element of the magnetic film, then the hysteresis losses in this element are expressed by (16).

$$[\oint BdH]_i = \frac{1}{2} \omega \mu_{Im} |H_{max,i}|^2 = \frac{s\omega^2 H_{max,i}^2}{2} \left[ \frac{\mu_p(\mu_p - \mu_r)}{s^2 + \omega^2 \mu_p^2} \right] \quad (16)$$

Thus the total hysteresis losses in the magnetic film are given by (17).

$$P_h = \frac{1}{V} \sum_{i=1}^{n_{film}} 2\pi r_{e,i} \Delta_i [\oint BdH]_i \quad (17)$$

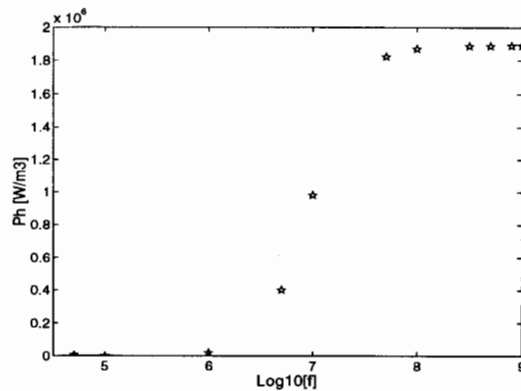
where  $n_{film}$  is the number of film finite elements,  $r_{e,i}$  the distance between the  $z$ -axis and the  $i^{\text{th}}$  element gravity center,  $\Delta_i$  the  $i^{\text{th}}$ -element surface.

The same decomposition goes for the eddy current losses on the film volume and (17) becomes:

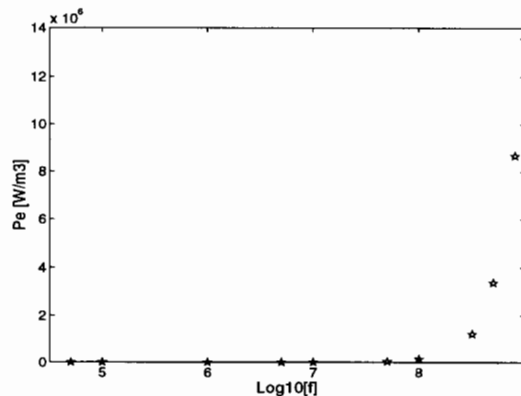
$$P_e = \frac{1}{V} \sum_{i=1}^{n_{film}} 2\pi r_{e,i} \Delta_i \sigma \omega^2 A_{e,i}^2 \quad (18)$$

where  $n_{film}$ ,  $r_{e,i}$ ,  $\Delta_i$  are defined above and  $A_{e,i}$  is the  $i^{\text{th}}$  element vector potential value at the gravity center.

Both losses are represented on Fig. 6 as a function of frequency.



a. Hysteresis losses



b. Eddy current losses

Fig. 6. Frequency characteristic of losses

#### 4.3. Discussion

Accounting for hysteresis is essential to model such PCB device and the permeability effect on the results can clearly be pointed out.

The skin depth is evaluated by the classical formula (16).

$$\delta = \sqrt{\frac{l}{\pi f \sigma \mu}} \quad (16)$$

In this expression, the permeability  $\mu$ , derived from the linearized Chua-type model, is a function of frequency. As shown in Fig. 2,  $\mu(f)$  decreases with frequency and then increases the skin depth value. The variations of the skin depth with frequency are represented in Fig. 7.

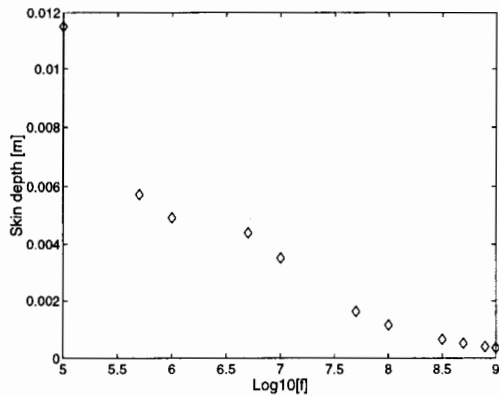


Fig. 7. Frequency variations of the skin depth  $\delta$

The skin depth decreases with frequency and takes, at the highest frequency of study  $f=1\text{GHz}$ , its lowest value  $\delta=360\mu\text{m}$  which is superior to the magnetic film thickness  $t_m=87.5\mu\text{m}$ . By consequence, eddy currents can be neglected and the magnetic behavior of the ferrite layer is essentially dominated by the complex permeability effect. In the frequency range, the magnetic field is then uniformly distributed in the film (Fig. 3) and the inductance keeps a quite constant value (Fig. 5).

According to (2), the permeability decreases and tends to the constant value  $\mu_r$  with increasing frequency. Thus the magnetic law becomes linear, giving rise to flat BH loops (Fig. 4). Furthermore, it can be deduced from (16) and (17) that high frequency hysteresis losses are proportional to the quantity

$$H_{max}^2 \left( 1 - \frac{\mu_r}{\mu_p} \right)$$

in each finite element. Neglecting the eddy currents makes the maximum value of the magnetic field and then the hysteresis losses constant, which is observed in Fig. 6. Moreover, this figure shows that hysteresis losses are dominating up to 500MHz whereas eddy current losses become major at this frequency.

By consequence, the modeling by the SDI method has made it possible to analyze the magnetic behavior of the device at high frequencies. The result analysis has shown the importance to account for hysteresis in the computation. The studied Mn-Zn ferrite thin film appeared to be suitable to reduce the electromagnetic

noise and to maintain good device performances at frequencies up to 1GHz.

## 5. CONCLUSION

In this paper, an original solving of a 2D unbounded PCB problem by the Strategic Dual Image method is presented. The modeled power layer is covered by a soft magnetic film, a Mn-Zn ferrite, and hysteresis is taken into account in the computation by using a linearized Chua-type model. The device behavior is simulated at high frequencies ranging from 0.1MHz to 1 GHz. The magnetic field distribution as well as typical characteristics are shown. Especially, the device inductance is increased by the ferrite layer and remains constant in the studied frequency range. This makes the Mn-Zn ferrite a suitable magnetic material for such high frequency applications and for the EMI control.

Two important points can enhance the quality of this modeling. Firstly, the dielectric characteristics of ferrite are neglected in this study. The consideration of the displacement currents will complete the physical description of the problem by studying the electric field distribution, the permittivity as well as the ohmic losses. Secondly, the 2D modeling permits to analyze accurately axisymmetric devices. However, PCB devices do not always present this symmetry. A 3D modeling is therefore required to study a wide choice of PCB configurations. This makes the object of further work.

## REFERENCES

- [1] F.Cortial, F.Ossart et. Al., "An improved analytical hysteresis model and its implementation in magnetic recording modeling by the finite element method", IEEE Trans. Magn, Vol.33, No.2, March 1997, pp. 1592-1595.
- [2] F.Cortial, "Modelisation de l'hysteresis et des dispositifs d'enregistrement magnetique", PhD thesis, Institut National Polytechnique de Grenoble, France, October 1996
- [3] S. Hayano, M. Namiki, and Y.Saito, "A magnetization model for computational magnetodynamics", J.Appl.Phys.,Vol.29, No.8, pp. 4614-4616 (April 1991).
- [4] S.Hayano, A.Miyazaki and Y.Saito, "Frequency characteristics of the complex permeability and its application to the FEM solution of hysteretic fields", J.Appl.Phys., Vol.69, No.8, pp. 4838-4840 (April 1991)
- [5] Y.Saito, K.Takahashi, and S.Hayano, "Finite element solution of unbounded magnetic field problem containing ferromagnetic materials" IEEE Trans. Magn, Vol.24, No.6, pp. 2946-2948 (November 1988).
- [6] K.Takahashi, Y.Saito and S.Hayano, "The strategic dual image method for the open boundary electromagnetic field problems" Int. J. Appl. El. Mat., Vol.4, pp. 178-184, 1993.
- [7] F. Cortial, S.Yoshida, H. Tohya, Y. Midorikawa and Y. Saito, "FEM analysis of PCB containing magnetic materials", MAG-97-117, Magnetics Society, The Institute of Electrical Engineering of Japan, July 1997.
- [8] E.C.Snelling, "Soft ferrites, properties and applications", Second Edition, Butterworths, 1988